

Journal Pre-proof

Adsorption of an anionic dye from aqueous solution on a treated clay

Maria C. Avila, Ileana D. Lick, Nora A. Comelli, Maria L. Ruiz

PII: S2352-801X(21)00145-4

DOI: <https://doi.org/10.1016/j.gsd.2021.100688>

Reference: GSD 100688

To appear in: *Groundwater for Sustainable Development*

Received Date: 4 June 2021

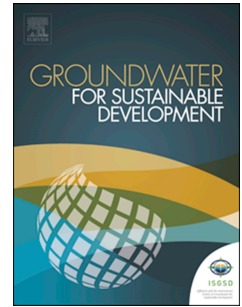
Revised Date: 5 October 2021

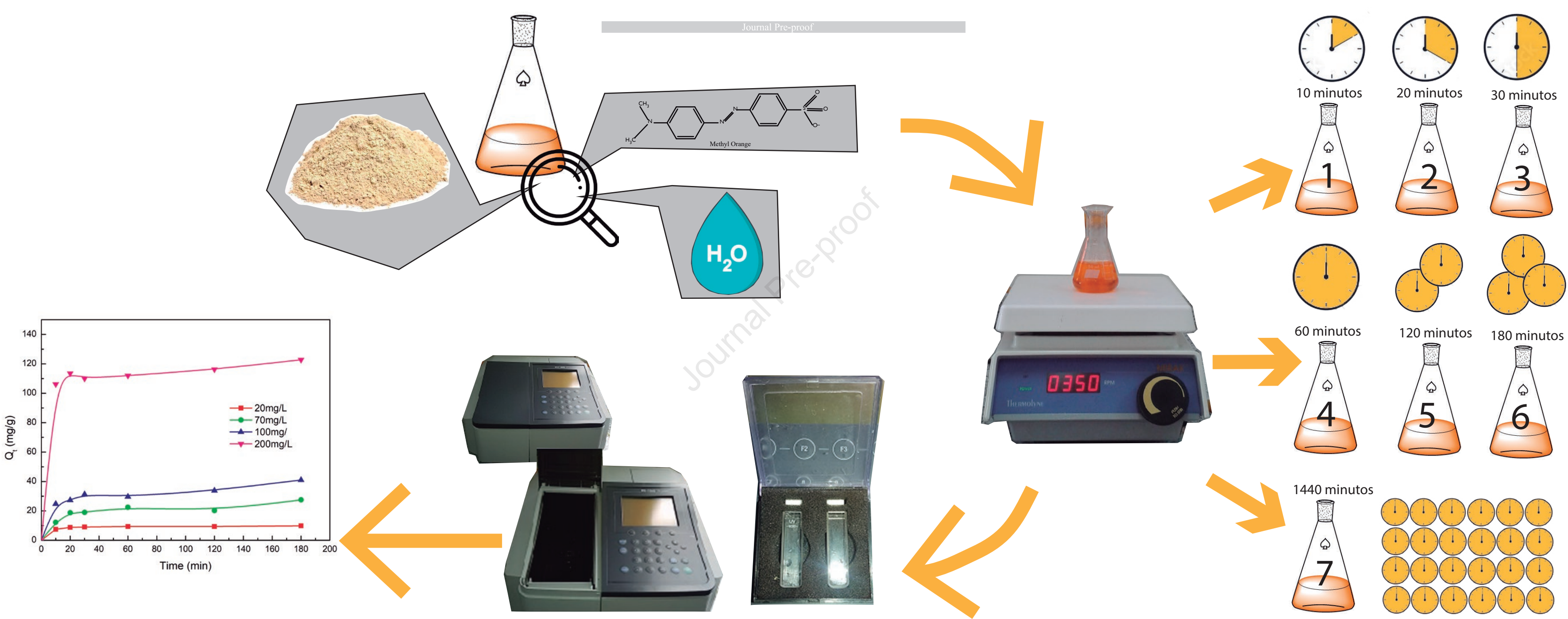
Accepted Date: 6 October 2021

Please cite this article as: Avila, M.C., Lick, I.D., Comelli, N.A., Ruiz, M.L., Adsorption of an anionic dye from aqueous solution on a treated clay, *Groundwater for Sustainable Development*, <https://doi.org/10.1016/j.gsd.2021.100688>.

This is a PDF file of an article that has undergone enhancements after acceptance, such as the addition of a cover page and metadata, and formatting for readability, but it is not yet the definitive version of record. This version will undergo additional copyediting, typesetting and review before it is published in its final form, but we are providing this version to give early visibility of the article. Please note that, during the production process, errors may be discovered which could affect the content, and all legal disclaimers that apply to the journal pertain.

© 2021 Elsevier B.V. All rights reserved.





Adsorption of an anionic dye from aqueous solution on a treated clay

Maria C. Avila^a, Ileana D. Lick^b, Nora A. Comelli^a, Maria L. Ruiz^a

^aINTEQUI-CONICET-UNSL. Facultad de Ingeniería y Ciencias Agropecuarias. Campus Universitario. Ruta Prov. N° 55 (Ex. 148) Extremo Norte. Villa Mercedes (San Luis) Argentina. mcavila@unsl.edu.ar

^bCINDECA-CONICET-UNLP. Facultad de Ciencias Exactas. Calle 47 N° 257, 1900 La Plata. Buenos Aires, Argentina.

Abstract

The presence of synthetic dyes in water causes serious environmental issues due to the poor water quality, toxicity to the environment and human carcinogenic effects. Adsorption has progressively become an economical and feasible method for dye wastewater decontamination. Clay minerals are an interesting alternative for removing colorants from colored aqueous solutions because they are inexpensive, easy to extract and handle, and non-toxic. In this work, a bentonite treated with H₂SO₄ is used to adsorb an azoderivative dye such as methyl orange (MO). The physicochemical properties of the solids were evaluated through X-ray powder diffraction (XRD), Brunauer Emmett Teller surface area analysis (BET), Scanning electron microscopy coupled with Energy dispersive spectroscopy (SEM-EDS), and Fourier transform infrared spectroscopy (FTIR). The initial dye concentration, adsorbent mass, contact time, temperature and pH influence the adsorption capacity. Acid modification of the clay increased its capacity to adsorb MO. For a concentration of 200 mg/L MO, an adsorption capacity of 125 mg/g was achieved. The adsorption process follows the pseudo second-order kinetic model. The thermodynamic study indicates that the adsorption is spontaneous and exothermic. The adsorption isotherm is best fitted to the Freundlich mathematical model. The results obtained show that, after receiving an acid treatment, clay can be effectively used to remove MO in aqueous solution.

Keywords: adsorption, clay, anionic dyes, isotherms, thermodynamic parameters, adsorption kinetics.

1. Introduction

Color is very important for our senses, as it determines the way in which we perceive the world. The color industry has grown considerably in recent years, as well as its toxicity. Today, water pollution by organic dyes resulting from the chemical and textile industry has attracted global attention due to the negative impact on public health [Bao *et al.*, 2011]. Generally, dyes are stable to light, heat and oxidizing agents [Wang and Zhu, 2006]. Likewise, dyes have a synthetic origin and a complex aromatic molecular structure that makes biodegradation more complicated [Ai *et al.*, 2011]. These substances have chromophore compounds with high molecular weight, which accumulate in water bodies, thus reducing luminosity and photosynthetic activity [McMullan *et al.*, 2001]. Additionally, most of the synthetic dyes affect the amount of dissolved oxygen, favoring eutrophication processes by increasing the organic load. The colored wastewater becomes the ecosystem in a dramatic source of aesthetic pollution and disturbance on aquatic life [Parsa *et al.*, 2007]. Furthermore, several dyes have carcinogenic and mutagenic effects on living beings [Aguiar *et al.*, 2015].

Dyes can be classified according to their functional group, charge and usefulness. Dyes classified by their chemical structure include azo, anthraquinone, indigoid, nitro, triarylmethane, etc., and based on their application, they may be classified as cationic dyes, anionic dyes (acid, reactive and direct), and non-ionic dyes (vat and disperse dye) [Pajak 2021; Zhou *et al.* 2019]. The most important feature of dyes is their charge, as it influences the efficiency of the adsorption process [Tan *et al.*, 2015]. A widely used dye from the azo group is MO, which also has very low biodegradability, rendering it a problem for the environment. Therefore, it is very important to subject the water courses containing this dye to some kind of treatment.

When treating wastewater from textile processes, the removal of dyes is one of the main objectives. However, since dyes were designed to be resistant to degradation by light or an oxidation agent, they are more difficult to remove by

conventional water treatment methods. Therefore, the methods used for this purpose need to evolve and improve constantly. Different methods have been studied and applied for the treatment of this type of wastewater, including chemical, biological, catalytic and physical processes. It is also very common to use a combination of these technologies [Hussein and Jasim 2021; Tianzhi *et al.* 2021; Dasgupta *et al.* 2017; Paredes-Quevedo *et al.* 2021; Dasgupta *et al.* 2016; Dasgupta *et al.* 2015; Hynes *et al.* 2020].

The methodologies classified as physical are considered to be inexpensive and simpler than the others. The adsorption process belongs to this category and has many advantages, such as the simplicity of its design and operation, its high performance and, most importantly, the fact that it is more inexpensive than other methods. In addition to its effectiveness in removing dyes from aqueous media, the adsorption strategy offers many advantages for industrial scales, such as its cost-benefit ratio, its rapid and straightforward protocol, the fact that the adsorbed dyes can be collected via desorption, among others [Saputra *et al.* 2021]. All these qualities make adsorption one of the most widely used methods for treating colored water [Shirazi *et al.* 2020, Chaari *et al.* 2021; Dehmani *et al.* 2021]. For the adsorption process to be a feasible, inexpensive and effective alternative, adsorbents are required. Among the most commonly used conventional adsorbent solids there is activated carbon, which works due to its excellent adsorption capacity. As disadvantages of this solid, we can mention its high cost and how complicated its regeneration process is [Liu *et al.*, 2019; España *et al.*, 2019]. As a result, in recent years several research groups have committed to studying and designing different adsorbent solids [Saputra *et al.* 2021, Lafi and Hafiane 2016; Li *et al.* 2018; Singh *et al.* 2018]. Hynes *et al.* (2020) classified adsorbents in general as organic and inorganic, regardless of whether they exhibit natural, synthetic, industry/agro/domestic waste properties. Within the group of natural materials, we find clays, an interesting option to be studied as an adsorbent. In modern life, clay minerals are one of the most important materials for a large number of industrial applications, and they are also the most abundant ones on Earth. Clays are used in the elimination and deposit of dangerous chemical products for the protection of the environment [Suryadi *et al.*, 2015; Sarkar *et al.*, 2019.]. They present a laminated structure, porosity, specific active sites, large surface area, high cation-

exchange capacity and thermal stability [Zhou *et al.*, 2019; Kausar *et al.*, 2018]. Clays can be modified to improve their adsorption capacities by subjecting them to various treatments, such as replacement of the cations present in the clay, thermal treatments, or acid treatments, in order to obtain solids that can be used for a specific pollutant [Sarkar *et al.* 2019; Gao *et al.* 2015; Yan *et al.* 2015; Satlaoui *et al.* 2019]. The purpose of inorganic acid modification is to enhance the adsorption capability of clay minerals by increasing the surface area, pore volume, and number of acid sites. The most widely used acid for this purpose is sulfuric acid (H_2SO_4), which is preferred over hydrochloric acid due to its lower cost and fewer detrimental effects [Suryadi *et al.*, 2015; Barakan and Aghazadeh 2021].

Bentonite is a rock composed of smectite (at least 50%), particularly montmorillonite with quartz, feldspar, gypsum and/or other minerals present as impurities [Martinez Stagnaro and Volzone 2019, Queiroga *et al.* 2019]. Bentonite is composed of two silica tetrahedral sheets with a central Al octahedral sheet. The permanent negative charge of bentonite was attributed to the isomorphous replacement of Al^{3+} with Si^{4+} in the tetrahedral layer, and of Mg^{2+} with Al^{3+} in the octahedral layer. This negative charge is balanced by the presence of exchangeable cations (Na^+ , Ca^{2+} , etc.) in the lattice structure, and these cations are exchangeable with inorganic and/or organic polycations, resulting in pillared materials, which enhance the adsorption of cationic, anionic and organic pollutants [Anirudhan and Ramachandran, 2015; Chinoune *et al.*, 2016]. As bentonite is highly available and environmentally safe, it seems to be an economical material for the removal of colorants. The only potential disadvantage of this material is its low affinity to adsorb anionic dyes due to its negative charge. Performing an acid treatment on a montmorillonite not only improves its adsorption capacity but also makes it suitable for retaining anionic dyes.

When studying the adsorption process of a dye, one of the main objectives is to find out the optimum operating parameters. For this purpose, numerical optimization is used to determine the quantities or values necessary for the different parameters to achieve maximum removal efficiency. These parameters include: pH, temperature, contact time, adsorbent mass and adsorbate concentration.

The problems caused by high levels of pollution make it clear that research to mitigate the damage is essential. Within the context of adsorption, the search for solids that work as adsorbents for highly contaminating dyes and that are highly effective is an ongoing enterprise. Finding inexpensive, natural and nature-friendly solids is very important. Additionally, in order to optimize the adsorption process, it is essential to study the parameters that affect the process, which are inherent and specific to each adsorbate/adsorbent system. Under this assumption, in this work, a natural bentonite and a treated one were characterized and studied as methyl orange adsorbents in an aqueous solution. The uptake time, initial concentration, sorbent dosage, pH and temperature effects were investigated, as well as the equilibrium, kinetics and thermodynamics.

2. Materials and Methods

2.1. Materials

Methyl orange (ucb) is an acid dye that, together with reactants and direct dyes, form the set of anionic dyes. This is commercially known as acid orange 52, azoderivated with color change from red to orange-yellow between pH 3.1 and 4.4. The indicator name is 4-Dimethylaminoazobenzene-4'-sulfonic Acid Sodium Salt. Nowadays, it is applied in pharmaceutical preparations, dyeing and oil processes.

The physical properties of methyl orange (MO) are shown in Table 1. For each experiment, MO solutions were prepared with distilled water.

The solid adsorbent used in this work is a low swelling magnesium calcium bentonite from San Juan (Argentina), which was supplied by Bentonitas Santa Gema. Natural clay (RC) was treated with concentrated sulfuric acid at 413 K in a pressure reactor, then it was washed to remove traces of acid, and finally the water content was removed by a spray dryer. The solid thus obtained is called treated clay (TC).

2.2. Methods

2.2.1. Characterization

The crystalline structure of solids was studied by X-ray diffraction (XRD) using a D-Max III (Rigaku) with Cu K α 1 radiation ($\lambda=1.5405 \text{ \AA}$, 40 kV, 30 mA), with Ni filter, and scanning an angular range of 2θ between 10° and 70° , at a 3°min^{-1} rate. The JCPDS (Joint Committee for Powder Diffraction Data-International Centre for Diffraction Data) database was used to analyze the diffraction peaks.

Fourier transformed infrared (FTIR) spectroscopy, Perkin-Elmer Spectrum RX1 analysis was performed in the range of $4000\text{-}400 \text{ cm}^{-1}$. The samples were ground with KBr (analytical grade) and the mixture was pressed to produce disks for the FTIR analysis.

The surface areas and pore volumes were determined from nitrogen adsorption isotherms measured at 77K in a Gemini V2.00 surface analyzer (Micromeritics Instrument Corp.).

The micrographs of the samples were obtained by scanning electron microscopy (SEM) using Philips 505 Model equipment provided with an EDAX DX PRIME 10 energy dispersive X-ray analyzer.

The Cation exchange capacity (CEC) is one of the important properties in clay minerals. It is a measure of the capacity of clay minerals to exchange cations from the solution. The CEC was obtained by the methylene blue method. The natural clay has a CEC of 95 meq/100g.

2.2.2. Adsorption Experiments

The experiments were carried out in a batch reactor with thermostatic bath. 50 mL of a colored solution with an initial concentration of dye (C_i) and with a mass of adsorbent (M) was used. It was stirred magnetically at 350 rpm. The samples were taken at different time intervals and the final concentration (C_t) was analyzed in an UV-visible spectrophotometer (UV-1800 SHIMADZU), where absorbance at maximum wavelength was evaluated. The calibration curve was performed in a concentration range for this work from 2 to 24 mg/L using the photometric method with UV-Probe Program.

To study the pH influence, it was adjusted to the desired value in a pH range of 3-10 at 298K, using a solution of 0.1 mol/L HCl (Merck) and 0.1 mol/L NaOH (Sigma-Aldrich, >97% w/w).

To measure the temperature effect, the experiments were conducted in a thermostatic bath at 298, 323 and 373 K. The adsorption capacity and the adsorption percentage were calculated using the following equations:

$$Q_t = (C_i - C_t) \frac{V}{M} \quad (1)$$

$$Removal\% = \left(1 - \frac{C_t}{C_i}\right) \cdot 100 \quad (2)$$

Where V is the volume of dye solution (L), C_i is the initial concentration of the dye solution (mg/L), C_t is the final concentration (mg/L), and M is the adsorbent mass (g).

The description of the adsorption procedure begins with the treated clay, and consist of several sequential steps, as explained in Figure 1.

3. Results and Discussion

3.1. XRD Analysis

The XRD pattern of adsorbent solids, RC and TC are present in Figure 2(a). It can be observed that the RC consists of montmorillonite as the main mineralogical phase, specifically a calcium-magnesium-hydrated aluminium silicate belonging to a montmorillonite-15A [ICDD PDF-2 00-003-0015]. In addition, it is noticeable the presence of minor amounts of cristobalite, quartz, feldspar and calcite. In the case of acid treated clay, the montmorillonite phase is preserved, indicating that it is resistant to acid attack.

The clays have a typical peak around $2\theta = 5^\circ$ [Yan *et al.*, 2015]. The natural clay which is studied in this work has a peak at $2\theta = 5.88^\circ$, similar to the cited one. When comparing the natural clay with the treated one, it can be seen that the angle 2θ has suffered a displacement of 5.88° to 5.17° respectively. The calculated distance d is 7.52 \AA (0.752 nm) and 8.55 \AA (0.855 nm) for RC and TC respectively, and this expansion suggests an exchange of ions. [Silva *et al.*, 2012; Koswojo *et al.*, 2010].

The XRD patterns of TC before and after reacting with MO are indicated in Figure 2(b). The value of 2θ for the diffractogram of clay with MO after adsorption (TC-MO) is 5.60, while for TC without adsorbed dye is 5.17. This shift towards higher values reveals an increase in the interlaminar spacing, caused by the MO retained in the clay.

3.2. FTIR Spectra

The IR spectrum of a clay mineral is dependent to its chemical composition, isomorphous substitution and layer arrangement order. Figure 3(a) shows the FTIR spectra of the RC and TC. The adsorption band at 3640 cm^{-1} represents the stretching vibration of the OH groups in the silicate layers; this band is attributed to the montmorillonite [Temuujin *et al.*, 2006; Aguiar *et al.*, 2017]. The band at 1640 cm^{-1} was assigned to the bending vibration of water. The RC exhibits a band with a maximum located about 1030 cm^{-1} and a shoulder at 1116 cm^{-1} assigned to the symmetric stretching vibration mode of Si-O-Si groups [Madejová, 2003].

The bands located at about 915 and 880 cm^{-1} , which are observed in RC and TC, are attributed to the bending vibration mode of Al-Al-OH and Al-Mg-Al respectively. These bands weaken in treated clay, suggesting that there is a partial Al and Mg reduction [Temuujin *et al.*, 2006]. Another characteristic band that increases its intensity in acid-treated clay is the 800 cm^{-1} band, which is attributed to amorphous silica. [Madejová, 2003]. The presence of bands at 520 and 470 cm^{-1} assigned to Si-O-Al (octahedral Al) and Si-O-Si [Madejová, 2003] suggests that the octahedral Al cations are retained and amorphous silica are observed respectively. This means that the original structure of the montmorillonite was not fully destroyed in agreement with the XDR result.

The FTIR method is extensively used to study the clay materials-organic intercalation. The FTIR spectra of MO and treated clay before the adsorption of dyes are shown in Figure 3(b). In the spectrum corresponding to dye, the band at 1609 cm^{-1} indicates the vibration of phenyl groups of MO anions. The bands at 1118 and 1200 cm^{-1} were attributed to the vibration of C-N of amines. The symmetric stretching

vibration of the SO_3^- group appears at 1038 cm^{-1} . The absorbance at 1006 cm^{-1} is due to the C-H bond corresponding to benzene rings. [El Hassani *et al.*, 2017]. These signals are defined in treated clay after the adsorption process, which would suggest that the MO molecules have been embedded in the surface of solid.

3.3. Textural Properties

The reason for the high adsorption capacity of clay is its high surface area. If a particular clay has an elevated surface area, this means that it has a high adsorption capacity compared to clays with a low surface area.

Both the natural and treated clay showed (Figure 4) a type V isotherm according to the ALOthman classification [ALothman 2012], which is typical of mesoporous materials (pore width from 2 nm to 50 nm). This isotherm is associated with capillary condensation occurring in mesopores, a limiting adsorption in an extended P/P_0 range and a monolayer multilayer adsorption at isotherm onset. The isotherm corresponding to the TC exhibits a hysteresis type H3 (IUPAC classification), which corresponds to a system formed by slot shaped pores having a vertical adsorption branch at relative pressures close to the unit, and a desorption branch at approximately medium pressure [Chinoune *et al.*, 2016].

From the parameters obtained for the RC and TC represented in Table 2, the effectiveness of the acid treatment applied to the clay in increasing the surface area (S_{BET}), pore size (D_p) and pore volume (V_p) was verified.

The surface area of TC increased significantly from 29.34 (natural clay) to $76.12\text{ m}^2/\text{g}$, which represents an increase of 160%. A similar situation occurred with the average pore volume, which went from 0.099 to $0.134\text{ cm}^3/\text{g}$, representing an increase of 35%. Acidification removes impurities, replacing interchangeable cations (like Na^+ , Ca^{2+}) with hydrogen ions and leaching other cations (Mg^{2+} , Al^{3+}) from the octahedral and tetrahedral sites produced by some damage on the silicate layer, which exposes the edges of platelets [Toor and Jin, 2012, Barakan and Aghazadeh 2021].

The good quality of an adsorbent is determined by its surface area and pore volume values. Both parameters are significantly improved in the modified solid (TC)

with respect to RC; therefore, the former would be expected to have a great ability to retain the dye.

On the other hand, the C_{BET} value is related to the monolayer adsorption enthalpy [Chinoune *et al.*, 2016]. An elevated C_{BET} value indicates a strong adsorbent-adsorbate interaction. Table 2 shows that this value is much higher for TC than RC, probably due to chemical changes during acid treatment.

3.4. Surface Morphology

The clay samples were examined using SEM and EDS to analyze their morphological characteristics with respect to the raw and treated bentonites. Herein, representative SEM images are present in Figure 5 (a) and (b), where there are noticeable differences between the two samples. In the image corresponding to natural clay (Fig. 5(a)), particles forming aggregates of different sizes are observed. In the case of treated clay (Fig. 5(b)), the size of the particles is smaller and homogeneously distributed, which is consistent with the results obtained with BET, which show a great increase in the surface area.

The results of EDS (Table 3) show semiquantitative quantities of O, Al and Si elements, which are part of the clay main structure. This table also includes Fe and K elements. Surface contents of Na, Mg and Ca disappear in the TC. The elemental mapping images are presented supplementary material Figure S1. The acid treatment carried out leads to a solid with a more porous surface due to the leaching of cations. This is because the bentonite cations are replaced by H^+ ions, generating empty spaces on the surface. This has resulted in a morphological modification of the clay physico-chemical surface, which would favor the process of dye adsorption. Saputra *et al.* (2021) argue that mesoporous properties, high surface area, and pore volume, as well as enrichment with functional groups are beneficial features provided by an adsorbent. The TC has all of these features.

The area of the treated bentonite has increased markedly with respect to the natural bentonite and, what is more, its surface has been morphologically modified in such a way that its dye-capturing capacity has been improved.

3.5. Effect acid treatment

To study the efficiency of solids adsorption, 50 mL of a MO solution with an initial concentration of 100 mg/L with 60 mg of natural and treated clay were subjected to magnetic stirring at room temperature. The percentage of dye removal is shown in Figure 6(a).

The TC has a high adsorption capacity to remove MO in aqueous solution with a removal rate of 86%, reaching equilibrium within 3 hours of contact. This clearly shows the marked difference between both solids in their behavior as adsorbents. The high removal percentage of the TC as compared to the little activity exhibited by the RC shows that the acid treatment performed on the natural bentonite is effective for removing an anionic dye.

3.6. Effect of pH

The pH of the solution plays an important role in modifying the medium in which the two phases meet: the colored solution and the surface of the solid adsorbent [Elmoubarki *et al.*, 2015].

The effect of pH on the adsorption was studied with 60 mg of adsorbent and an initial MO concentration of 100 mg/L. Experiments were carried out during 10, 20, 30, 60, 120 and 180 minutes at a constant stirring rate. The results are shown in Figure 6(b).

The graph proves that the mass of MO adsorbed per mg of TC, Q_t , is high at an acidic pH and then decreases slightly as the pH increases, although this reduction is very slow until a pH value of 7 is reached. As long as protons slowly disappear from the solution, the adsorption capacity reaches a maximum of 42 mg/g at pH 4.

Two adsorption mechanisms are possible: electrostatic interactions between the surface groups of the clays and the functional groups of the dye molecule, and/or a chemical reaction between the clays and the dye [Elmoubarki *et al.* 2015, Singh *et al.*, 2018].

These adsorption mechanisms could be explained, on the one hand, because the MO molecule is protonated at a pH below pK_a (3.47). Figure 6(c) shows the positively and negatively charged species of MO according to pH. At a pH equal to

or greater than 3.2, the protonated ion predominates, forming two resonant structures, one of which is a double-charged zwitterion. When the pH increases until it reaches the pK_a of the dye, the amount of H^+ decreases, thus generating a deprotonated MO, and it remains like this even at an acidic pH of 4.4. At pH values close to the pK_a , the molecule is deprotonated, thus reaching a negative charge and becoming an anion [Seyhan Ege, 2013].

At low pH values, the dissociated species of the MO are attracted by the positively charged surface of the solid through electrostatic interactions that take place between the double positive and negative charge of the MO of the resonant forms. This double charge present in the zwitterion has an additional electrostatic interaction, which is relevant for the removal of the azo dye. When the hydroxyl concentration increases, the dye has a persistent negative charge on the sulfonic group, thus generating a hydrogen bridge between the oxygen of the sulfonic group and the protons of the hydroxyls present on the clay surface.

On the other hand, the adsorption for MO molecules is high due to the formation of the cation π interaction between the positively charged surface of the TC and partial negative charge of the aromatic rings within the MO molecular structure.

When the pH begins to increase, the removal of the MO decreases dramatically until it becomes non-existent at alkaline pH. The TC surface becomes deprotonated and negatively charged. At this point, a gradual decline of the MO adsorption takes place as the result of the partial ionization of the sulfonic group within the MO structure, thus creating the anionic form of MO that leads to the electrostatic repulsion with the surface of the acidic bentonite [Ong *et al.*, 2014].

The weak adsorption of the anionic dye at alkaline pH could be attributed to the abundance of hydroxyl ions, OH^- , which compete with the anionic dye for the same adsorption sites [Elmoubarki *et al.* 2015].

Based on the explanation above, it is suggested that the removal of the azo dye is increased at an acidic pH. The results of this study are consistent with the work carried out by other researchers in determining how the electrostatic attraction

occurs between the adsorbent solid and the dye [Zhou *et al.* 2010, Umpuch *et al.* 2013, Pajak, 2021, Dadou *et al.*, 2019].

3.7. Effect of Contact Time and Dye Concentration

The effect of contact time and initial concentration of the dye was studied using different concentrations of dye: 20, 70, 100 and 200 mg/L. Experiments were carried out using 60 mg of TC at different contact times (0-180 min), at 298 K and pH 4. Each sample was centrifuged to separate the remaining solid from the solution. The supernatant liquid was optically measured in the UV.

Figure 6(d) depicts how the adsorption capacity of the TC is modified with the range of selected initial concentrations of the azo dye. The experimental results show that the TC quickly removes the MO. The adsorption capacity increases from 12 to 125 mg/g when the initial concentration increases from 20 to 200 mg/L of MO. The initial concentration values decline when the stirring time increases. The increase of molecules in the solution is the driving force that enhances removal over time. A higher initial concentration of MO promotes the overcoming of the resistance to mass transfer between this species in the solution and the solid phase. As a result, with an increase in the initial concentration, there is also a decrease in the concentration of MO in the solution within a certain period of time, thus resulting in an improvement in the adsorption process.

For all the initial concentrations, the adsorption capacity increases when the stirring time increases. Removal of the MO increases as the contact time between the solid and the colored solution elapses. During the first 20 minutes after the adsorption process is started, MO removal is fast, the curves at any C_i have a high slope, which evinces strong adsorption. After 20 minutes, the evolution of adsorption is progressive but slow, until equilibrium is reached at approximately 180 minutes.

3.8. Effect of Amount of Adsorbent

Yagub *et al.* (2014) explain that the adsorbent dose is an important parameter of the process to determine the capacity of an adsorbent under certain operating conditions. Generally, the percentage of removed dye rises with the increase in adsorbent concentration, due to the greater number of adsorption sites that will be

available. The influence of the amount of adsorbent gives an idea of the ability to remove a dye. Using less adsorbent is economically beneficial.

In this study, the adsorption of MO was performed using 70 mg/L, at 298 K and pH 4, varying the amount of adsorbent used in a range of 5-100 mg. Figure 6(e) shows that as the concentration of adsorbent increases, the removal of MO increases, because a greater amount of TC means there are more active sites to attract the pollutant. Mohammed *et al.* (2021) published similar conclusions.

For the lowest concentrations used (0.04 and 0.1g/L) no changes were recorded in the dye spectrum. Regarding doses higher than 1.2 g/L and 2.0 g/L, the removal percentage was 48% and 75%, respectively (Figure 6(e) and 6(f)). It is then proven that the color of the MO solution fades as the adsorbent mass increases, which means that the removal efficiency increases. An opposite effect is observed with an increase in the mass of dye per gram of adsorbent (Q_t), wherein 28 and 26 mg/L are obtained for the same doses (1.2 and 2.0 g/L). This may be attributed to the formation of aggregates of the adsorbent solid, which implies that the sites for the adsorption of the MO block each other, thus reducing the available surface area and causing a reduction in Q_t as a result. This behavior was also observed by Saeed *et al.* (2020) and Chinoune *et al.* (2016).

3.9. Adsorption Kinetics

Figure 7 shows the adsorption kinetics under the following conditions: 100 mg/L of C_i and 60 mg of TC. It evidences that it takes approximately 3 hours to reach equilibrium.

To study the rate of adsorption, the adsorption kinetics of MO on the adsorbent solid was analyzed using two kinetic models on the experimental results at various initial concentrations of the dye. The Pseudo First (3) and Pseudo Second (4) Order Models are represented in the following way:

$$\ln(Q_e - Q_t) = \ln Q_e - k_1 t \quad (3)$$

For pseudo-first order kinetics (equation 3), the kinetic parameters were calculated using the $\ln(Q_e - Q_t)$ graph as a function of t . For this purpose, a nonlinear regression was performed with MATLAB software. From this, it was obtained k_1 (1/min), and the theoretical Q_e (mg/g). Whereas, for the pseudo-second order

equation, the kinetic parameters resulted from the graph of t/Q_t as a function of t , where Q_e [mg/g] and k_2 [g/mg-min] were calculated from the slope and the ordinate to the origin respectively.

$$\frac{t}{Q_t} = \frac{1}{kQ_e^2} + \frac{1}{Q_e}t \quad (4)$$

By linearizing this expression, $\frac{1}{kQ_e^2}$ is called h , from which the value of the constant k of adsorption velocity can be obtained. The results suggest that the removal of dye is done by a pseudo-second order model. Equation (4) is based on the assumption of a chemical mechanism in which the speed-controlling step is a chemisorption or an activation process. The different data obtained (maximum adsorption capacity, pseudo-second velocity constant and first order and linear regression coefficient) are grouped in Table 4.

Generally, the values of the constant rate of adsorption of the treated clay decreased with the increase of the initial MO concentration. The calculated Q_e values were very similar to those obtained experimentally. The results obtained indicate that the pseudo-second order Ho model fits better (R^2 about 1).

3.10. Adsorption Isotherms

Unbalanced and unsaturated molecular forces are present on the surface of a solid. When the solid comes into contact with a solute, interaction forces appear; the surface of the solid tends to balance the residual forces by attracting and retaining the solute molecules on its surface. This results in a high concentration in the surface neighborhood compared to the concentration in the fluid. In adsorption, it must be clear that two types of forces are involved: physical forces (dipolar momentum, polarization forces, dispersive forces or short-distance repulsive interactions) and chemical forces (involving chemical reactions and interactions responsible for the formation of chemical compounds). The adsorption of MO onto TC at different temperatures is determined as a function of equilibrium dye concentration (C_e) and the corresponding adsorption isotherms are plotted in Figure 8(a). The adsorption isotherms were performed in a concentration range (20-1000 mg/L) and at three temperatures: 298, 323 and 373 K. Initially, a gradual increase in the amount of

adsorbed dye (Q_e) is observed, followed by a moderate increase for higher concentration values. The Q_e decreases with an increase in temperature, which specifies an exothermic nature of the existing process.

The relationship between the amount of solute on the surface of an adsorbent in equilibrium with the concentration of the solute in the liquid phase defines the equilibrium of the adsorption process, and it is important for understanding the adsorption process itself. This equilibrium process is described by Adsorption Isotherms, whose equations were originally developed for the description of gas phase absorption processes. However, these can be used for liquid phase adsorption by applying the corresponding approximations in each case. The most commonly used equations for correlation of experimental adsorption data for hazardous substance systems-mineral clays are Langmuir and Freundlich. There are also equations that involve a greater number of parameters such as: Dubinin-Radushkevich, Temkin, Toth, Slips, BET, among others. The adsorption isotherms receive a strong influence of temperature. Depending on whether it is high or low, the amount adsorbed will be lower or higher, depending on whether it is a physi-adsorption or chemi-adsorption. The results are presented in Figures 8(b)-8(d) and the parameters of the isotherms are presented in Table 5. By discussing about isotherm constants, it can be determined whether an adsorption system is favorable or unfavorable.

The Langmuir isotherm assumes that adsorption occurs in a monolayer on the surface containing a finite number of adsorption sites without transmigration of adsorbate on the surface plane [Langmuir, 1916]. This phenomenon is expressed in the following way:

$$\frac{C_e}{Q_e} = \frac{1}{Q_m} C_e + \frac{1}{Q_m K_L} \quad (5)$$

Where C_e is the concentration of adsorbate in equilibrium (mg/L), Q_e is the amount of adsorbate adsorbed per unit of adsorbent mass in equilibrium (mg/g), K_L is the Langmuir adsorption constant (L/mg), and Q_m is the theoretical maximum amount adsorbed on a monolayer on a surface containing a finite number of identical sites, per unit of adsorbed mass (mg/g). For the Langmuir isotherm, the following results

are obtained by linearizing equation (5), where C_e/Q_e vs C_e is plotted. Therefore, Q_m is obtained from the slope and K_L is obtained from the ordinate to the origin.

The characteristics of this equation can also be expressed in terms of a dimensionless factor defined as (6):

$$R_L = \frac{1}{1+K_L C_o} \quad (6)$$

The R_L value indicates the type of isotherm obtained; favorable ($0 < R_L < 1$), not favorable ($R_L > 1$), linear ($R_L = 1$) or irreversible ($R_L = 0$). Table 5 shows that the R_L values are between 0 and 1 so that the adsorption of MO onto treated clay is favorable.

On the other hand, Freundlich isotherm [Freundlich, 1907] takes into account heterogeneous systems and is not restricted to the formation of the monolayer. This isotherm is expressed in the following way:

$$\ln Q_e = \ln K_F + \frac{1}{n} \ln C_e \quad (7)$$

Where K_F is a distribution coefficient expressing the amount absorbed per unit of adsorbent equilibrium concentration, and n provides an indication of how favorable the adsorption process is, both are the Freundlich constants. According to the result of Table 5 the MO/TC system shows an adsorption moderately difficult [Ong *et al.*, 2014].

The Dubinin-Radushkevich (D-R) isotherm model does not assume a homogenous surface or constant adsorption potential as other models [Chen *et al.*, 2011]. The D-R isotherm has been written by the following equations:

$$Q_e = Q_m e^{-B\varepsilon^2} \quad (8)$$

$$\varepsilon = RT \ln \left(1 + \frac{1}{C_e} \right) \quad (9)$$

$$E_a = (2B)^{-\frac{1}{2}} \quad (10)$$

Where B is a constant related to the adsorption energy, Q_m is the theoretical saturation capacity, and ε is the Polanyi potential.

From the equations (8-10), E_a can be calculated, the values of which are presented in Table 5. The values of E_a at different temperatures are between 5 and 8 KJ/mol for the three temperatures studied. The average energy of adsorption is the change of free energy when a mole of ions is transferred from the solution to the

surface of the solid. The values of this parameter can give information about the adsorption mechanism: in a range of 1 to 8 kJ/mol, they show physical adsorption [Onyango *et al.*, 2004]; between 8 and 16 kJ/mol, they indicate that the adsorption process is by ion exchange; while if the values are between 20 and 40 kJ/mol, they indicate chemisorption [Tahir and Rauf, 2006]. According to the values shown in Table 5 the MO/TC system would indicate a physical adsorption.

By comparing the correlation coefficients R^2 , it can be deduced that the experimental equilibrium adsorption data are well described by the Freundlich equation compared with Langmuir and D-R models.

3.11. Effect of Temperature on Adsorption

On the other hand, the process of adsorption in equilibrium is related to variables that are not possible to measure directly through the thermodynamics of the process, such as ΔH° (standard enthalpy change), ΔS° (standard entropy change), and ΔG° (Gibbs free energy), which is the most important of all. ΔG° expresses whether the adsorption process is possible or not, that is to say, whether the process is spontaneous or not.

The diffusion of the adsorbate molecules through the outer surface and internal pores of the adsorbing particles is affected by temperature. In order to study the effect of temperature on the dye/TC system, the following experiments were carried out with a C_i of 100 mg/L, with an adsorbent mass of 60 mg of TC at different temperatures (298K, 323K and 373K) and at different stirring times (20, 60, 120 and 180 min). Figure 6(g) shows how the effect of temperature influences the time that sorbent and dye are together. It is observed that the removal percentage decreases with increasing temperature.

Thermodynamic parameters such as Gibbs G° free energy, standard enthalpy H° and standard entropy S° were studied to better understand the effect of temperature on adsorption. The thermodynamic parameters were studied using equations (11) and (12):

$$\ln K_D = \frac{\Delta S^\circ}{R} - \frac{\Delta H^\circ}{RT} \quad (11)$$

$$K_D = \frac{Q_e}{C_e} \quad (12)$$

Where the ideal gas constant is $R=8.314$ J/mol K, T is the temperature in Kelvin and K_D is the distribution coefficient. The graph of $\ln K_D$ vs $1/T$ gives a straight line, and the slope and the ordinate to the origin correspond to $\Delta H^\circ/R$ and $\Delta S^\circ/R$ respectively.

The free energy values of Gibbs ΔG° at different temperatures were obtained from:

$$\Delta G^\circ = \Delta H^\circ - T\Delta S^\circ \quad (13)$$

$$\Delta G^\circ = -RT \ln K_D \quad (14)$$

The results are detailed in Table 7. Negative ΔG° values at different temperatures indicate the feasibility of the process and the spontaneous nature of the adsorption, and when the temperature increases, the ΔG° values increase, which shows that the adsorption is lower at high temperatures.

3.12. Comparison of adsorption processes for methyl orange removal

Table 7 compares the maximum adsorption capacities (Q_{\max}) of other research papers with different solid adsorbents for MO. Different parameters have been considered, such as: initial concentration, pH, adsorbent mass, and time, because Q_{\max} is dependent on them.

Various adsorbents have been used and continue to be designed to remove methyl orange from a colored solution. A great variety of solids, from natural clays, organic waste, coals and zeolites, have been modified by different acid, basic and thermal treatments.

A group of clays treated with sulfuric or hydrochloric acid were found to be good adsorbents to remove MO; they have a maximum adsorption capacity ranging from 10 to 47 mg/g [Fernandes *et al.* (2020), Bendaho *et al.* (2017), Ma *et al.* (2013)]. Other clays of the zeolite type were modified by Raador *et al.* (2021) with hexamethylenediamine (HMDA), improving the positive charge of the surface and causing the MO adsorption performance to increase as a result. Similar materials modified with organic compounds, such as the solids worked on by Zayed *et al.* (2018) and Chen *et al.* (2011), attained an advantageous removal capacity for the MO/adsorbent system. Other more complex adsorbents were also found in the

literature, e.g.: chitosan-kaolin with the addition of Fe composites [Zhu *et al.*, 2010] and chitosan-modified clay from Umpuch *et al.*, (2013), which yielded significant results but had the disadvantage that large amounts of the solid or a great amount time were needed to accomplish the removal, which is unfavorable from an economic standpoint. Gamoudi and Srasra (2019), experimented with a clay modified with a surfactant and achieved an adsorption efficiency of 100 mg/g within one hour of stirring and with an initial concentration of 200 mg/L of MO. All of these works provide evidence of an acceptable adsorption capacity; however, the solid studied in this work has been shown to have a better performance. The maximum adsorption capacity was determined to be about 125 mg/g, and this result was better than those adsorbents reported in the Table 7.

In summary, the bentonite from San Juan modified with sulfuric acid proposed in this work as an adsorbent has many advantages for removing MO.

4. Conclusions and Recommendation

The results obtained in this work show that clay from San Juan, Argentina, after receiving an acid treatment, can be effectively used to remove an anionic dye in aqueous solution. Analytical characterization techniques led to the conclusion that acid treatment modifies the morphological surface of natural clay, favoring the adsorption process. An initial concentration of the azo dye (20-1000 mg/L) with a mass of the acidified bentonite (5-100mg) were contacted in a batch reactor. At 298 K, the adsorption capacity of the TC increases with an increasing C_i for the same mass of the solid. The pH of the colored solution has a decisive impact on the adsorption process caused by the pK_a value of the MO. When the concentration of H^+ begins to increase, removal reaches a peak and then drops dramatically at alkaline pH. The adsorption process followed the pseudo second order rate kinetic. The Ho model is the best-fitted one, with an R^2 close to 1, which predicts the way in which adsorption occurs. The adsorption isotherm for MO/TC system is best fitted by Freundlich. This fit indicates an adsorption process wherein removal takes place by means of physical adsorption, through electrostatic interactions between species with opposite charges. The thermodynamic study indicates that the adsorption is

spontaneous and exothermic. The process cost for dye removal by adsorption depends mainly on the cost of the adsorbent. The bentonite studied here is an excellent choice for its abundance, easy handling and low cost when treated to improve its efficiency. This solid adsorbent has a promising future to improve the treatment of effluents from the textile industry. Therefore, it would be a great opportunity to continue the research on the influence of other chemical compounds present in aqueous waste such as acids, bases, mordants or other dyes. In this way, the TC would be studied in conditions closer to reality.

Acknowledgements

We thank the School of Engineering and Agricultural Sciences (*Facultad de Ingeniería y Ciencias Agropecuarias*) of the National University of San Luis (*Universidad Nacional de San Luis*), the Research Institute of Chemical Technology (*Instituto de Investigación en Tecnología Química, INTEQUI*) and the Applied Sciences Development and Research Center (*Centro de Investigación y Desarrollo en Ciencias Aplicadas, CINDECA*)-National Scientific and Technical Research Council (*Consejo Nacional de Investigaciones Científicas y Técnicas de Argentina, CONICET*). To Dr. Sandra Mosconi for the FTIR. To Dr. Jorge Gonzales for carrying out the XRDs.

References

- Aguiar, J.E.; Cecilia, J.A.; Tavares, P.A.S.; Azevedo, D.C.S.; Rodríguez Castellón, E.; Lucena, S.M.P.; Silva Junior, I.J. 2017. Adsorption study of reactive dyes onto porous clay heterostructures. *App. Clay Sci.* 135, 35–44. <https://doi.org/10.1016/j.clay.2016.09.001>
- Aguiar, J.E.; De Oliveira, J.C.A.; Silvino, P.F.G.; Neto, J.A.; Silva Jr., I.J.; Lucena, S.M.P. 2015. Correlation between PSD and adsorption of anionic dyes with different molecular weights on activated carbon. *Colloids Surf. A Physicochem. Eng. Asp.* 496,125–131. <https://doi.org/10.1016/j.colsurfa.2015.09.054>
- Ai, L.; Zhang, C.; Liao, F.; Wang, Y.; Li, M.; Meng, L.; Jiang J. 2011. Removal of methylene blue from aqueous solution with magnetite loaded multi-wall carbon nanotube: Kinetic, isotherm and mechanism analysis. *J. Hazard. Matter.* 198, 282 – 290. <https://doi.org/10.1016/j.jhazmat.2011.10.041>

ALothman, Z.A. 2012. Review: fundamental aspects of silica mesoporous materials. *Materials* 5, 2874 – 2902. <https://doi.org/10.3390/ma5122874>

Anirudhan, T.S.; Ramachandran, M. 2015. Adsorptive removal of basic dyes from aqueous solutions by surfactant modified bentonite clay (organoclay): Kinetic and competitive adsorption isotherm. *Process Saf. Environ. Prot.* 9 5, 215–225. <http://dx.doi.org/10.1016/j.psep.2015.03.003>

Bao, N.; Li, Y.; Wei, Z.; Yin, G.; Niu, J. 2011. Adsorption of dyes on hierarchical mesoporous TiO₂ fibers and its enhanced photocatalytic properties, *J. Phys. Chem. C.* 115, 13, 5708 - 5719. <https://doi.org/10.1021/jp1100939>

Barakan, S. Aghazadeh, V. 2021. The advantages of clay mineral modification methods for enhancing adsorption efficiency in wastewater treatment: a review. *Environ. Sci. Pollut. Res.* 28, 2572–2599. <https://doi.org/10.1007/s11356-020-10985-9>

Bendaho, D.; Driss, T. A.; Bassou D. 2017. Adsorption of acid dye onto activated Algerian clay. *Bull. Chem. Soc. Ethiop.* 31, 51-62. <http://dx.doi.org/10.4314/bcse.v31i1.5>.

Chaari, I.; Medhioub, M.; Jamoussi, F.; Hamzaoui, A. H. 2021. Acid-treated clay materials (Southwestern Tunisia) for removing sodium leuco-vat dye: Characterization, adsorption study and activation mechanism. *J. Mol. Struct.* 1223, 128944. <https://doi.org/10.1016/j.molstruc.2020.128944>

Chen, H.; Zhao, J.; Wu, J.; Dai, G. 2011. Isotherm, thermodynamic, kinetics and adsorption mechanism studies of methyl orange by surfactant modified silkworm exuviae. *J. Hazard Mater.* 192, 246– 254. <https://doi.org/10.1016/j.jhazmat.2011.05.014>

Chinoune, K.; Bentaleb, K.; Bouberka, Z.; Nadim, A.; Maschke, U. 2016. Adsorption of reactive dyes from aqueous solution by dirty bentonite. *App. Clay Sci.* 123, 64–75. <https://doi.org/10.1016/j.clay.2016.01.006>

Dadou, S.; Berrama, T.; Doufene, N.; Zekkaoui, C.; Beriber, A. 2019. Evaluating Untreated Clay's Adsorptive Capacity to Remove an Anionic Dye from Aqueous Solution. *Arab. J. Sci. Eng.* 44, 9889–9903. <https://doi.org/10.1007/s13369-019-04100-5>.

Dasgupta, J.; Sikder, J.; Chakraborty, S.; Adhikari, U.; Reddy B. V. P.; Mondal A.; Curcio, S. 2017. Microwave-Assisted Modified Polyimide Synthesis: A Facile Route to the Enhancement of Visible-Light-Induced Photocatalytic Performance for Dye Degradation. *ACS Sustainable Chem. Eng.* 5, 8, 6817–6826. <https://doi.org/10.1021/acssuschemeng.7b01044>.

Dasgupta, J.; Singh, A.; Kumar, S.; Sikdera, J.; Chakraborty, S.; Curcio, S. 2016. Hassan A. Arafat. Poly (sodium-4-styrenesulfonate) assisted ultrafiltration for methylene blue dye removal from simulated wastewater: Optimization using response surface methodology. *J. Environ. Chem. Eng.* 4, 2008–2022. <http://dx.doi.org/10.1016/j.jece.2016.03.033>.

- Dasgupta, J.; Singh, M.; Sikder, J.; Padarthy, V.; Chakraborty, S.; Curcio, S. 2015. Response surface-optimized removal of Reactive Red 120 dye from its aqueous solutions using polyethyleneimine enhanced ultrafiltration. *Ecotoxicol. and Environ. Saf.* 121, 271–278. <http://dx.doi.org/10.1016/j.ecoenv.2014.12.041>.
- De Queiroga, L. N. F.; França, D. B.; Rodrigues, F.; Santos, I. M.G., Fonseca, M. G.; Jaber, M. 2019. Functionalized bentonites for dye adsorption: Depollution and production of new pigments. *J. Environ. Chem. Eng.* 7, 103333. <https://doi.org/10.1016/j.jece.2019.103333>
- Dehmani, Y.; El Khalki, O.; Mezougane, H.; Abouarnadasse, S. 2021. Comparative study on adsorption of cationic dyes and phenol by natural clays. *Chem. Data Collect.* 33, 100674. <https://doi.org/10.1016/j.cdc.2021.100674>.
- El Hassani, K.; Beakou, B. H.; Kalnina, D.; Oukani, E.; Anouar A. 2017. Effect of morphological properties of layered double hydroxides on adsorption of azo dye Methyl Orange: A comparative study. *App. Clay Sci.* 140, 124–131. <https://doi.org/10.1016/j.clay.2017.02.010>
- Elmoubarki, R.; Mahjoubi, F. Z.; Tounsadi, H.; Moustadraf, J.; Abdennouri, M.; Zouhri, A.; El Albani, A.; Barka, N. 2015. Adsorption of textile dyes on raw and decanted Moroccan clays: Kinetics, equilibrium and Thermodynamics. *Water Resour. Ind.* 9, 16-29. <https://doi.org/10.1016/j.wri.2014.11.001>.
- España, V. A. A.; Sarkar, B.; Biswas, B.; Rusmirc, R.; Naidu, R. 2019. Environmental applications of thermally modified and acid activated clay minerals: Current status of the art. *Environ. Technol. Innov.* 13, 383–397. <https://doi.org/10.1016/j.eti.2016.11.005>.
- Fernandes, J.V.; Rodrigues, A.M.; Menezes, R.R.; Neves, G.d.A. 2020. Adsorption of Anionic Dye on the Acid-Functionalized Bentonite. *Materials.* 13, 3600. <https://doi.org/10.3390/ma13163600>.
- Freundlich, H., 1907. Über die Adsorption in Lösungen. *Zeitschrift. Physikalische Chemie (Leipzig)* 57U, 385–470. <https://doi.org/10.1515/zpch-1907-5723>.
- Gao, Z.; Li, X.; Wu, H.; Zhao, S.; Deligeer, W.; Asuha, S. 2015. Magnetic modification of acid-activated kaolin: Synthesis, characterization, and adsorptive properties. *Micropor. Mesopor. Mater.* 202, 1–7. <http://dx.doi.org/10.1016/j.micromeso.2014.09.029>.
- Gamoudi, S.; Srasra, E. 2019 Adsorption of organic dyes by HDPyP-modified clay: Effect of molecular structure on the adsorption. *J. Mol. Struct.* 1193, 522-531. <https://doi.org/10.1016/j.molstruc.2019.05.055>
- Hussein, T. K.; Jasim, N. A. 2021. A comparison study between chemical coagulation and electrocoagulation processes for the treatment of wastewater containing reactive blue dye. *Mater. Today: Proc.* 42, 1946–1950. <https://doi.org/10.1016/j.matpr.2020.12.240>.
- Hynes, N. R. J.; Kumar, J. S.; Kamyab, H.; Sujana, J. A. J; Al-Khashman, O. A.; Kuslu, Y.; Ene, A.; Kumar, B. S. 2020. Modern enabling techniques and adsorbents based dye removal with

- sustainability concerns in textile industrial sector -A Comprehensive review. *J. Clean. Prod.* 272, 122636. <https://doi.org/10.1016/j.jclepro.2020.122636>.
- Kausar, A.; Iqbal, M.; Javed, A.; Aftab, K.; Nazli, Z.; Haq Nawaz Bhatti, Shazia Nouren. 2018. Dyes adsorption using clay and modified clay: A review. *J. Mol. Liq.* 256, 395-407. <https://doi.org/10.1016/j.molliq.2018.02.034>.
- Koswojo, R.; Pramudhita Utomo, R.; Ju, Y.-H.; Ayucitra, A.; Soetaredjo, F. E.; Sunarso, J.; Ismadji, S. 2010. Acid Green 25 removal from wastewater by organo-bentonite from Pacitan. *App. Clay Sci.* 48, 81–86. <https://doi.org/10.1016/j.clay.2009.11.023>
- Lafi, R.; Hafiane, A. 2016. Removal of methyl orange (MO) from aqueous solution using cationic surfactants modified coffee waste (MCWs). *J. Taiwan Inst. Chem. Eng.* 58, 424–433. <http://dx.doi.org/10.1016/j.jtice.2015.06.035>.
- Langmuir, I. 1916. The constitution and fundamental properties of solids and liquids. Part I. Solids. *J. Am. Chem. Soc.* 38, 2221-2295. <https://doi.org/10.1021/ja02268a002>
- Li, B.; Wang, Q.; Guo, J.-Z.; Huan, W.-W.; Liu, L. 2018. Sorption of methyl orange from aqueous solution by protonated amine modified hydrochar. *Bioresour. Technol.* 268, 454–459. <https://doi.org/10.1016/j.biortech.2018.08.023>.
- Liu, M.; Li, X.; Du, Y.; Han, R. 2019. Adsorption of methyl blue from solution using walnut shell and reuse in a secondary adsorption for Congo red. *Bioresour. Technol. Rep.* 5, 238-242. <https://doi.org/10.1016/j.biteb.2018.11.006>
- Ma, Q.; Shen, F.; Lu, X.; Bao, W.; Ma, H. 2013. Studies on the adsorption behavior of methyl orange from dye wastewater onto activated clay. *Desalin. Water Treat.* 51, 3700-3709. [https://doi:10.1080/19443994.2013.782083](https://doi.org/10.1080/19443994.2013.782083)
- Madejová, J. 2003. FTIR techniques in clay mineral studies. *Vibrat. Spec.* 31,1-10. [https://doi.org/10.1016/S0924-2031\(02\)00065-6](https://doi.org/10.1016/S0924-2031(02)00065-6)
- Martinez Stagnaro, S. Y.; Volzone, C. 2019. Adsorption of anionic dyes monoazo and diazo using organo-bentonites. *SN Appl. Sci.* 1, 70. <https://doi.org/10.1007/s42452-018-0070-3>.
- McMullan, G.; Meehan, C.; Conneely, A.; Kirby, N.; Robinson, T.; Nigam, P.; Banat, I.M.; Marchant, R.; Smyth, W.E. 2001. Microbial decolourisation and degradation of textile dyes. *Appl. Microbiol. Biotechnol.* 56, 81 – 87. <https://doi.org/10.1007/s002530000587>
- Mohammed, A. A.; Kareem S. L. 2021. Enhancement of ciprofloxacin antibiotic removal from aqueous solution using ZnO nanoparticles coated on pistachio shell. *Desalin. Water Treat.* 213, 229-239. <http://doi:10.5004/dwt.2021.26674>
- Ong, L.K.; Soetaredjo, F.E.; Kurniawan, A.; Ayucitra, A.; Liu, J.-C.; Ismadji, S. 2014. Investigation on the montmorillonite adsorption of biocidal compounds incorporating thermodynamical-based

multicomponent adsorption isotherm. *Chem. Eng. Sci.* 241, 9-18. <https://doi.org/10.1016/j.ces.2013.12.001>.

Onyango, M.S.; Kojima, Y.; Aoyi, O.; Bernardo, E.C.; Matsuda, H. Adsorption equilibrium modeling and solution chemistry dependence of fluoride removal from water by trivalent-cation-exchanged zeolite F-9. 2004. *J. Colloid Interface Sci.* 279, 341–350. <https://doi.org/10.1016/j.jcis.2004.06.038>.

Pajak, M. 2021. Adsorption Capacity of Smectite Clay and Its Thermal and Chemical Modification for Two Anionic Dyes: Comparative Study. *Water Air Soil Pollut.* 232, 83. <https://doi.org/10.1007/s11270-021-05032-3>

Paredes-Quevedo, L. C.; González-Caicedo, C.; Torres-Luna, J. A.; Carriazo, J. G. 2021. Removal of a Textile Azo-Dye (Basic Red 46) in Water by Efficient Adsorption on a Natural Clay. *Water Air Soil Pollut.* 232:4. <https://doi.org/10.1007/s11270-020-04968-2>.

Parsa J.B., Abbasi M. 2007. Decolorization of synthetic and real wastewater by indirect electrochemical oxidation process. *Acta Chim. Slov.* 54, 792 - 796. [URN:NBN:SI:DOC-I9BVIJP6](https://doi.org/10.1007/s11270-020-04968-2)

Radoor, S.; Karayil, J.; Jayakumar, A.; Parameswaranpillai, J.; Siengchin, S. 2021. Efficient removal of methyl orange from aqueous solution using mesoporous ZSM-5 zeolite: Synthesis, kinetics and isotherm studies. *Colloids Surf. A* 611, 125852. <https://doi.org/10.1016/j.colsurfa.2020.125852>

Saeed, M.; Munir, M.; Nafees, M.; Shoib, S.; Shah, A.; Ullah, H.; Waseem, A. 2020. Synthesis, characterization and applications of silylation based grafted bentonites for the removal of Sudan dyes: Isothermal, kinetic and thermodynamic studies. *Micropor. Mesopor. Mater.* 291, 109697. <https://doi.org/10.1016/j.micromeso.2019.109697>.

Saputra, O. A.; Nauqinida, M.; Kurnia, Pujiasih, S., Kusumaningsih, T., Pramono, E. 2021. Improvement of anionic and cationic dyes removal in aqueous solution by Indonesian agro-waste oil palm empty fruit bunches through silylation approach. *Groundw. Sustain. Dev.* 13, 100570. <https://doi.org/10.1016/j.gsd.2021.100570>

Sarkar, B.; Rusmin, R.; Ugochukwu, U. C.; Mukhopadhyay R.; Manjaiah, K. M. 2019. Modified Clay and Zeolite Nanocomposite Materials: Environmental and Pharmaceutical Applications. Chapter 5. Elsevier. 113-127. <https://doi.org/10.1016/B978-0-12-814617-0.00003-7>.

Satlaoui, Y.; Trifi, M.; Fkih Romdhane, D.; Charef, A.; Azouzi, R. 2019. Removal Properties, Mechanisms, and Performance of Methyl Green from Aqueous Solution Using Raw and Purified Sejnane Clay Type. *J. Chem.* Article ID 4121864, 15 pages. <https://doi.org/10.1155/2019/4121864>

Seyhan Ege. 2013. *Organic Chemistry. Structure and Reactivity. Volume 2.* Editorial Reverté S. A.

Shirazi, E. K.; Metzger, J. W.; Fischer, K.; Hassani, A. H. 2020. Removal of textile dyes from single and binary component systems by Persian bentonite and a mixed adsorbent of bentonite/charred dolomite. *Colloids Surf. A.* 598, 124807. <https://doi.org/10.1016/j.colsurfa.2020.124807>.

- Silva, M. M. F.; Oliveira, M. M.; Avelino, M. C.; Fonseca, M. G.; Almeida, R. K. S.; Silva Filho, E. C. 2012. Adsorption of an industrial anionic dye by modified-KSF-motmorillonite: Evaluation of the kinetic, thermodynamic and equilibrium data. *Chem. Eng. J.* 203 (2012) 259-268. <https://doi.org/10.1016/j.cej.2012.07.009>
- Singh, N.B.; Nagpal, G.; Agrawal, S; Rachna. 2018. Water purification by using Adsorbents: A Review. *Environ. Technol. Inno.* 11,187–240. <https://doi.org/10.1016/j.eti.2018.05.006>
- Suryadi Ismadji, Felycia Edi Soetaredjo, Aning Ayucitra.2015. *Clay Materials for Environmental Remediation* Springer International Publishing. <https://doi.org/10.1007/978-3-319-16712-1>
- Tahir, S.S.; Rauf, N. 2006. Removal of cationic dye from aqueous solutions by adsorption onto bentonite clay. *Chemosphere.* 63, 1842–1848. <https://doi.org/10.1016/j.chemosphere.2005.10.033>
- Tan, K. B.; Vakili, M.; Horri, B. A.; Poh, P. E.; Abdullah, A. Z.; Salamatinia, B. 2015. Adsorption of dyes by nanomaterials: Recent developments and adsorption mechanisms. *Sep. Purif. Technol.* 150, 229-242. <https://doi.org/10.1016/j.seppur.2015.07.009>
- Temuujin, J.; Senna, M.; Jadambaa, T.; Burmaa, D.; Erdenechimeg S.; MacKenzie, K. 2006. *J. Chem. Technol. Biotechnol* 81: 688-693. <https://doi.org/10.1002/jctb.1469>
- Tianzhi, W.; Weijie, W.; Hongying, H.; Khu, S-T. 2021. Effect of coagulation on bio-treatment of textile wastewater: Quantitative evaluation and application. *J. Clean. Prod.* 312, 127798. <https://doi.org/10.1016/j.jclepro.2021.127798>
- Toor, M.; Jin, B. 2012. Adsorption characteristics, isotherm, kinetics, and diffusion of modified natural bentonite for removing diazo dye. *Chem. Eng. Sci.* 187, 79-88. <https://doi.org/10.1016/j.cej.2012.01.089>
- Umpuch C. and Songsak S. 2013. Removal of methyl orange from aqueous solutions by adsorption using chitosan intercalated montmorillonite. *Songklanakarin J. Sci. Technol.* 35 (4), 451-459.
- Wang, S.; Zhu, Z.H. 2006. Characterization and environmental application of an Australian natural zeolite for basic dye removal from aqueous solution, *J. Hazard. Mater.* 136, 946 – 952. <https://doi.org/10.1016/j.jhazmat.2006.01.038>
- Yagub, M. T.; Sen, T. K.; Afroze, S.; Ang, H. M. 2014. Dye and its removal from aqueous solution by adsorption: A review. *Adv. Colloid Interface Sci.* 209, 172-184. <https://doi.org/10.1016/j.cis.2014.04.002>
- Yan, L.; Qin, L.; Yu, H.; Li S., Shan, R.; Du, B. 2015. Adsorption of acid dyes from aqueous solution by CTMAB modified bentonite: Kinetic and isotherm modeling. *J. Mol. Liq.* 211,1074–1081. <https://doi.org/10.1016/j.molliq.2015.08.032>
- Zayed, A. M.; Abdel Wahed, M. S.M.; Mohamed, E. A.; Sillanpää, M. 2018. Insights on the role of organic matters of some Egyptian clays in methyl orange adsorption: Isotherm and kinetic studies. *App. Clay Sci.* 166, 49–60. <https://doi.org/10.1016/j.clay.2018.09.013>

Zhou, Y.; Lu, J.; Zhou, Y.; Liu, Y. 2019. Recent advances for dyes removal using novel adsorbents: A review. Environ. Pollut. 252, 352-365. <https://doi.org/10.1016/j.envpol.2019.05.072>

Zhu, H-Y.; Jiang R.; Xiao L. 2010. Adsorption of an anionic azo dye by chitosan/kaolin/ γ -Fe₂O₃ composites. App. Clay Sci. 48, 522-526. <https://10.1016/j.clay.2010.02.003>

Journal Pre-proof

Table 1: Chemical Composition and physics properties of dye

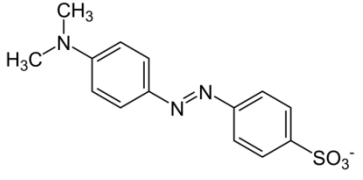
	Methyl orange
Structure	
Molecular Formula	C ₁₄ H ₁₄ N ₃ NaO ₃ S
Molecular Weight	327.34 g/mol
Type	Ionic, anionic, azo dye
CAS number	547-58-0
Color Index	13025
λ_{max}	464
pK_a	3.47 (25°C)

Table 2. Results obtained from BET analysis.

	Raw Clay	Treated Clay
BET surface area (m ² /g)	29.34	76.11
BJH pore volume (cm ³ /g)	0.099	0.134
Pore size (Å)	12.46	73.50
C _{BET}	136.53	899.54

Table 3. EDS analysis surface atomic contents of clays

Element	Raw Clay Atomic %	Treated Clay Atomic %
O	49.94	56.57
Na	2.03	n.d.
Mg	2.51	n.d.
Al	10.53	12.81
Si	33.05	29.17
K	0.22	0.58
Ca	1.02	n.d.
Fe	0.70	0.87

Table 4: Kinetic Parameters

C_i (mg/L)	Pseudo Second Order			Pseudo First Order		
	k₂	Q_e (mg/g)	R²	k₁	Q_e (mg/g)	R²
70	6.53 .10 ⁻³	11.64	0.99973	0.0479	9.8812	0.977
100	2.04 .10 ⁻³	28.05	0.99949	0.0479	24.5755	0.9216
200	2.36 .10 ⁻⁴	70.77	0.99491	0.0406	45.59	0.8031

Table 5: Parameters of the isotherms Langmuir, Freundlich and Dubinin-Radushkevich

		298K	323K	373K
Langmuir	Q_m	467.289	456.621	215.517
	K_L	0.00322	0.00223	0.00276
	R_L	0.23696	0.30959	0.26595
	R²	0.77534	0.79792	0.65863
	SD	0.38992	0.39293	1.53913
Freundlich	K_F	2.85071	1.545735	0.49038
	n	1.26708	1.173846	1.01196
	R²	0.92462	0.94441	0.88879
	SD	0.48512	0.42263	0.66851
Dubinin-Raduschkevich	Q_m	155.888	154.3248	140.016
	B	0.00767	0.01224	0.01996
	E_a	8.0739	6.3913	5.0050
	R²	0.80271	0.8808	0.92992
	SD	0.7595	0.6087	0.5364

Table 6: Thermodynamic adsorption parameters

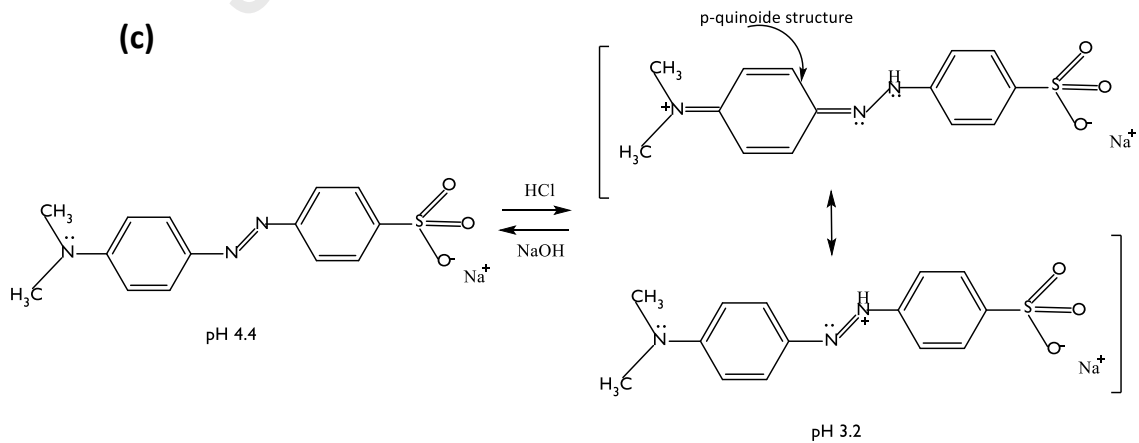
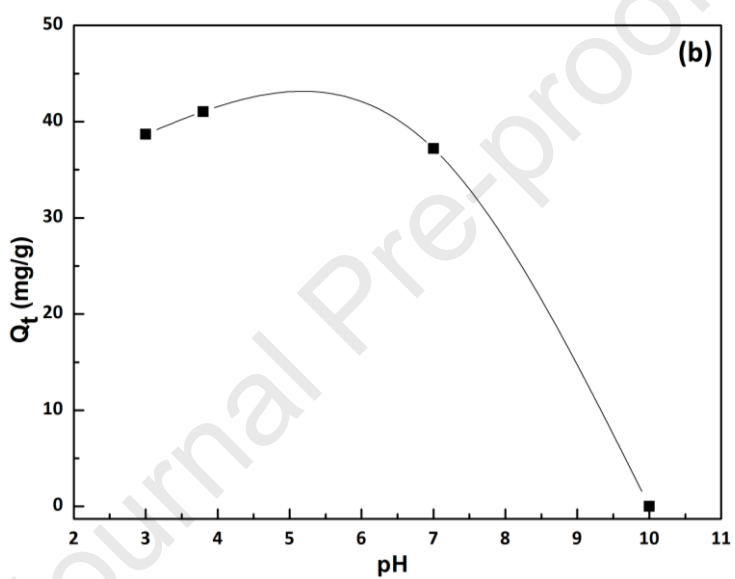
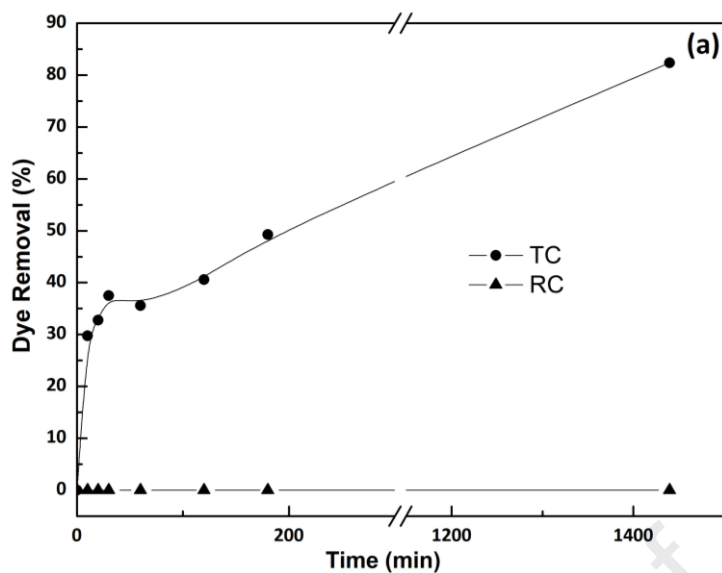
Dye Concentration (mg/L)	ΔH° (KJ/mol)	ΔS° (J/mol K)	ΔG° (KJ/mol K)		
			298K	323K	373K
20	-25.34	-79.66	-1.57	0.33	4.39
70	-2.97	-12.36	0.73	0.98	1.65
100	-13.11	-45.05	0.52	1.06	3.85
200	-15.60	-45.03	-2.09	-1.22	1.26
300	-25.78	-8.56	-0.88	-0.23	1.05
400	-16.20	-5.33	-0.51	-0.10	0.70
500	-23.52	-6.91	0.10	0.68	1.86
1000	-14.14	-52.94	1.918	2.45	5.82

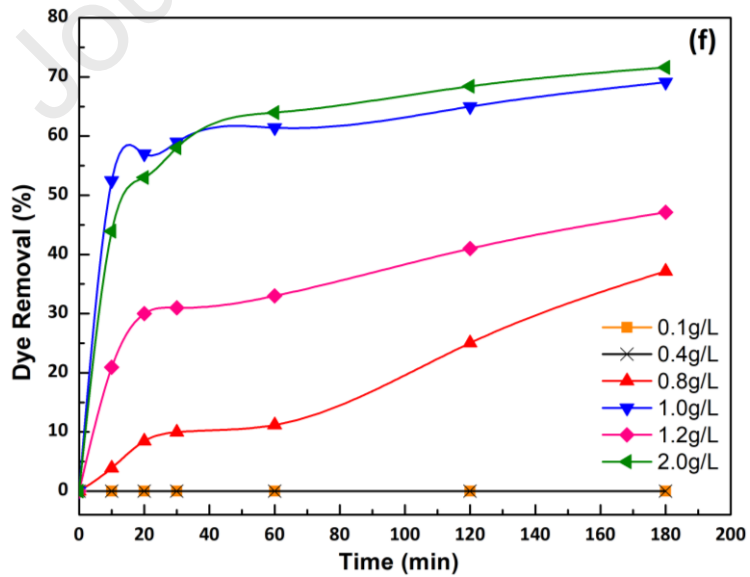
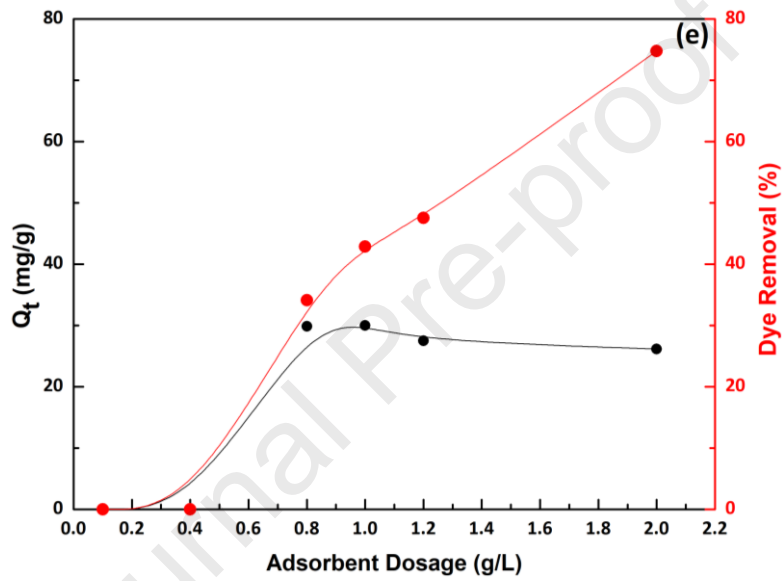
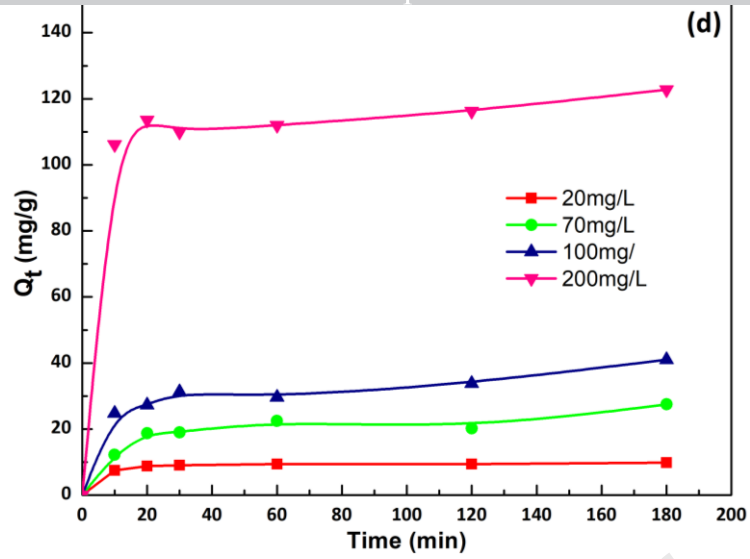
Table7: Comparison of the Q_{max} of MO dye by various adsorbents

Adsorbents	C_i (mg/L)	pH	Adsorbent Mass (g)	Time(min)	Q_e (mg/g)	Reference
Bentonite modified	50	6	0.1	240	47.8	Fernandes et al. (2020)
Activated clay	26.2	(a)	0.08	30	10	Bendaho et al.(2017)
Activated clay	80	7	0,5	120	11	Ma et al. (2013)
Mesoporous zeolite	10	1	0.12	260	5	Radoor et al. (2021)
Organic- matter rich clay	100	2	0.1	240	24	Zayed et al. (2018)
Surfactant modified silkworm	300	4	0.05	60	78	Chen et al. (2011)
Chitosan- caolin	20	(a)	0.05	240	100	Zhu et al. (2010)
Arcilla- chitosan	200	7	0.1	60	96	Umpuch et al.(2013)
Modified clay	200	(b)	0.1	60	100	Gamoudi and Srasra (2019)
Bentonite modified	200	4	0,06	180	125	This work

(a) date not specificated

(b) independen adsorption of pH





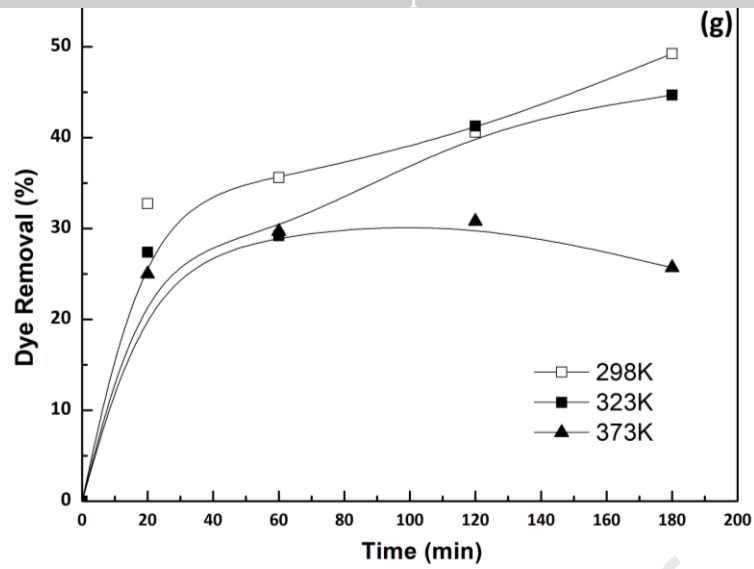


Figure 6. Influence of experimental factors: **(a)** acid treatment; **(b)** pH; **(c)** MO at different pH values [Seyhan Ege, 2013]; **(d)** contact time (min) and MO initial concentration; **(e)** adsorbent mass; **(f)** contact time (min) and adsorbent concentration; **(g)** temperature.

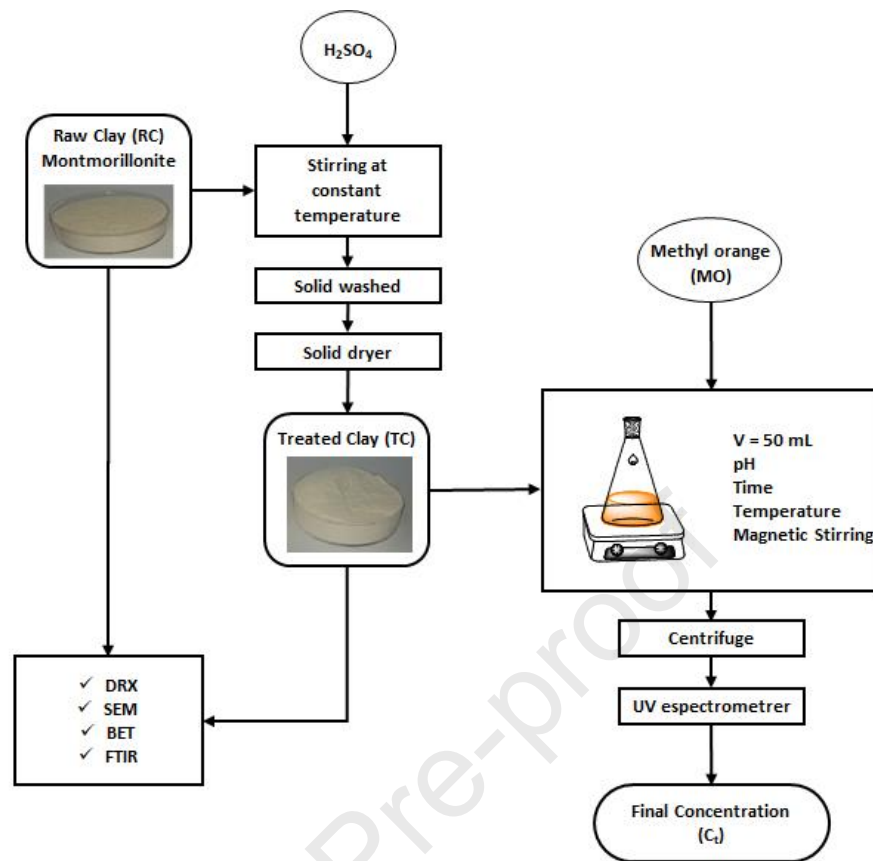


Figure 1. Flowchart of the adsorption process.

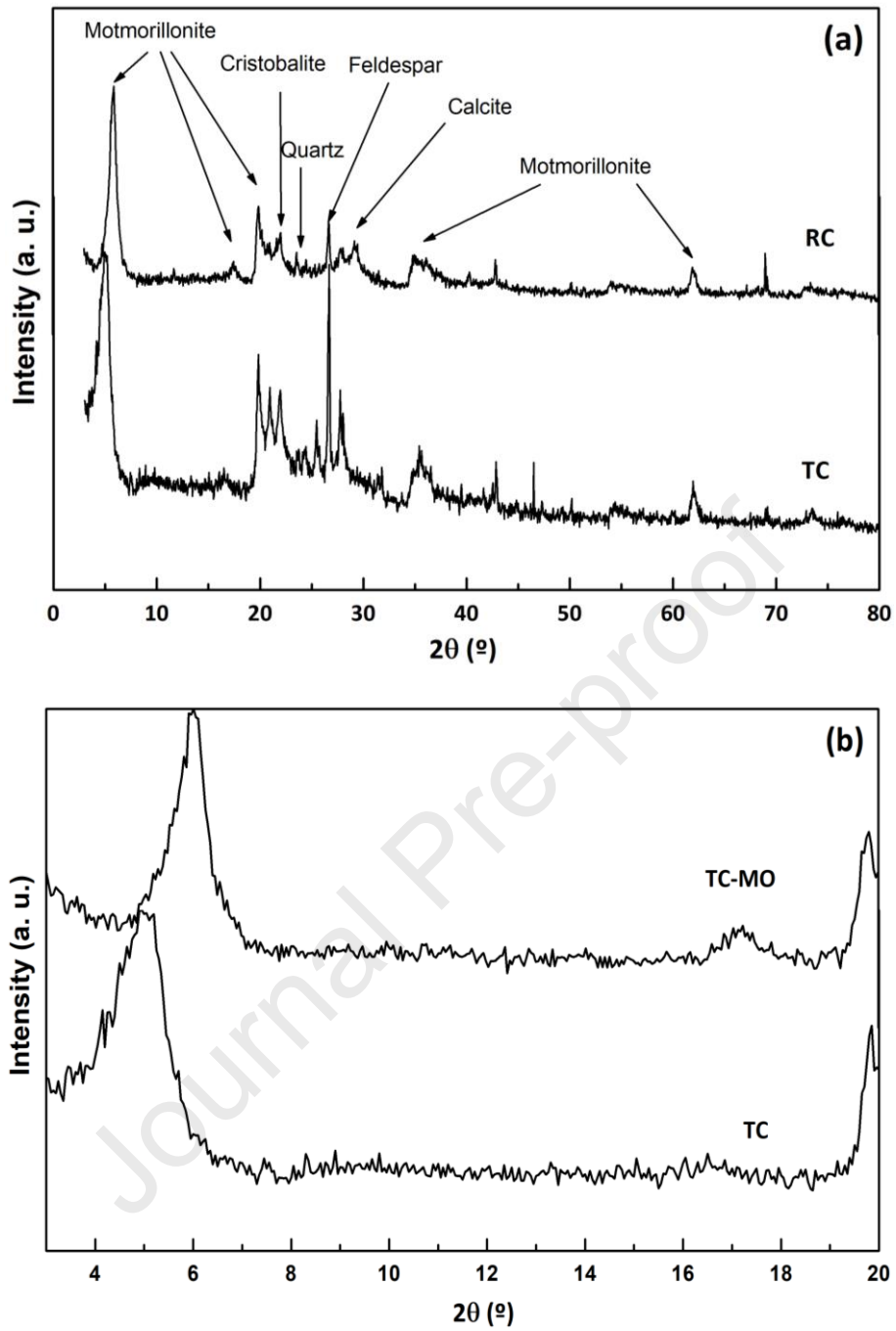


Figure 2. XRD patterns: (a) RC and TC; (b) TC and TC-MO after adsorption.

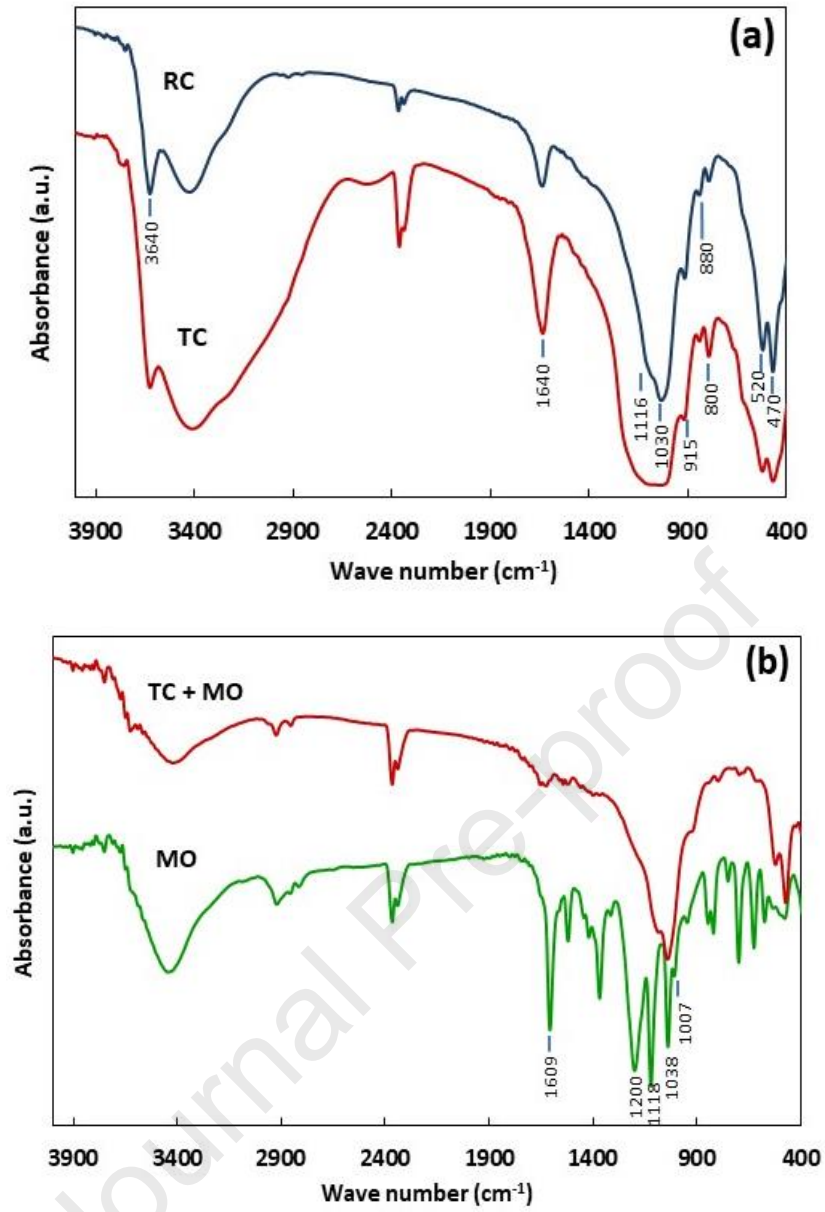


Figure 3. FTIR spectra: (a) RC and TC; (b) MO and TC after adsorption.

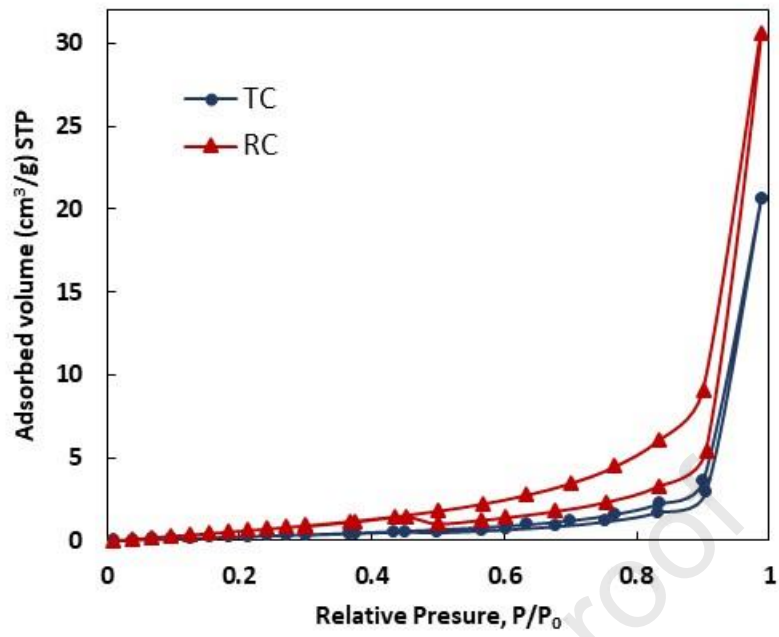


Figure 4. N_2 adsorption–desorption isotherms of RC and TC.

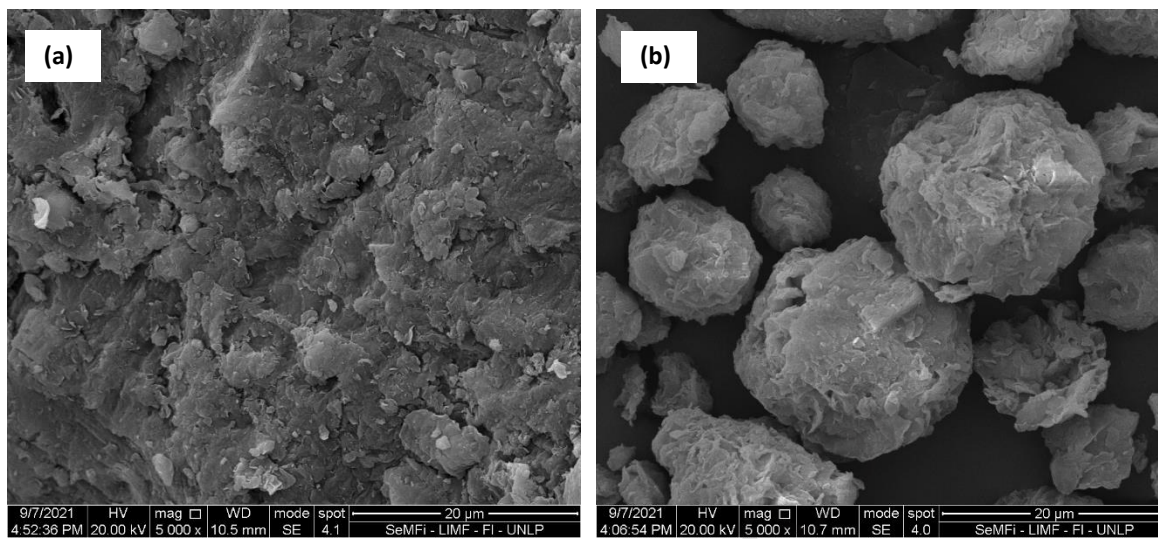


Figure 5. SEM micrographs of clays: (a) raw, (b) treated.

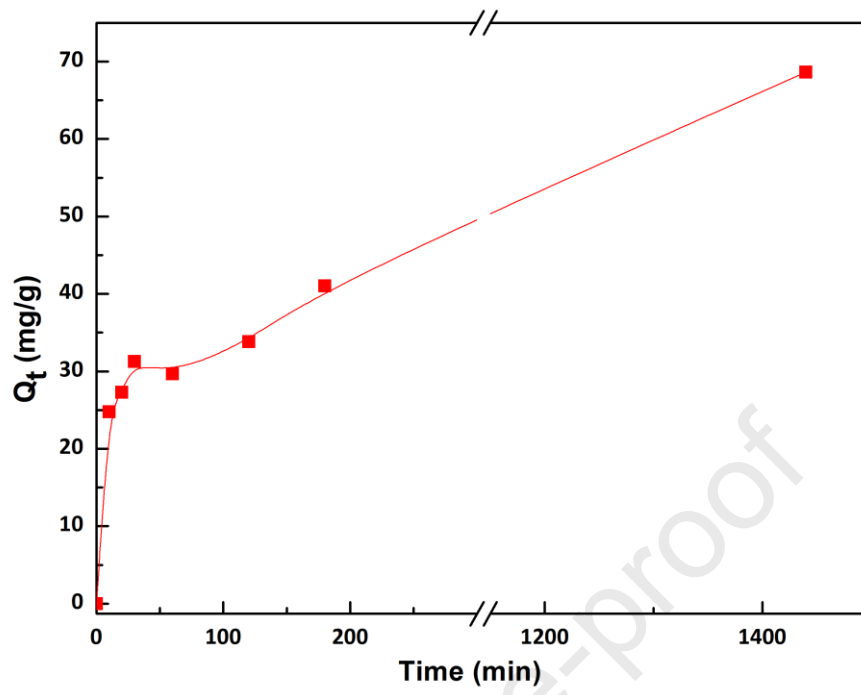
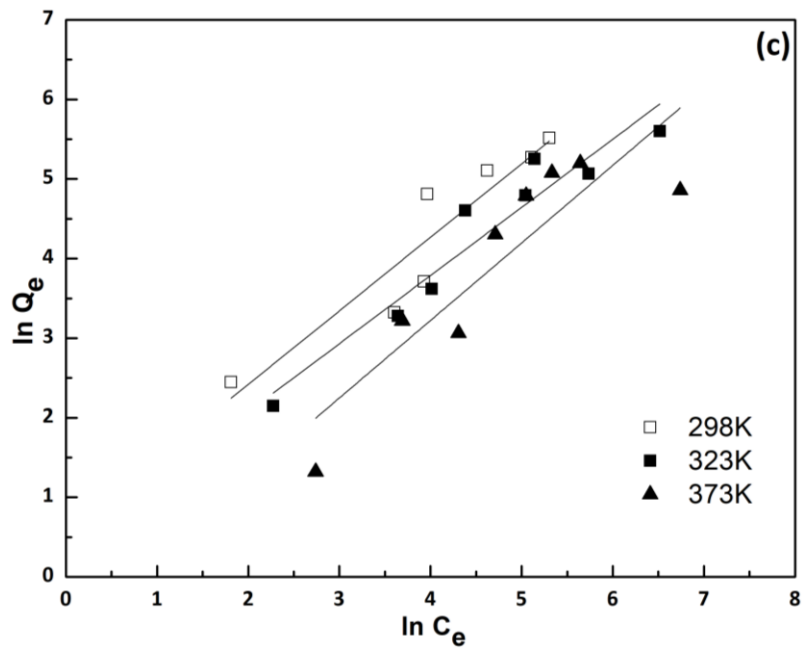
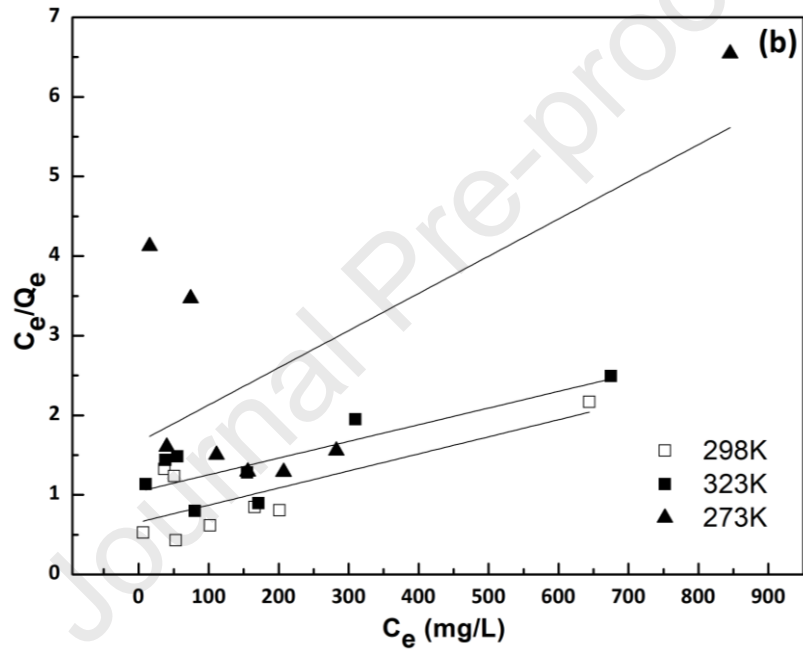
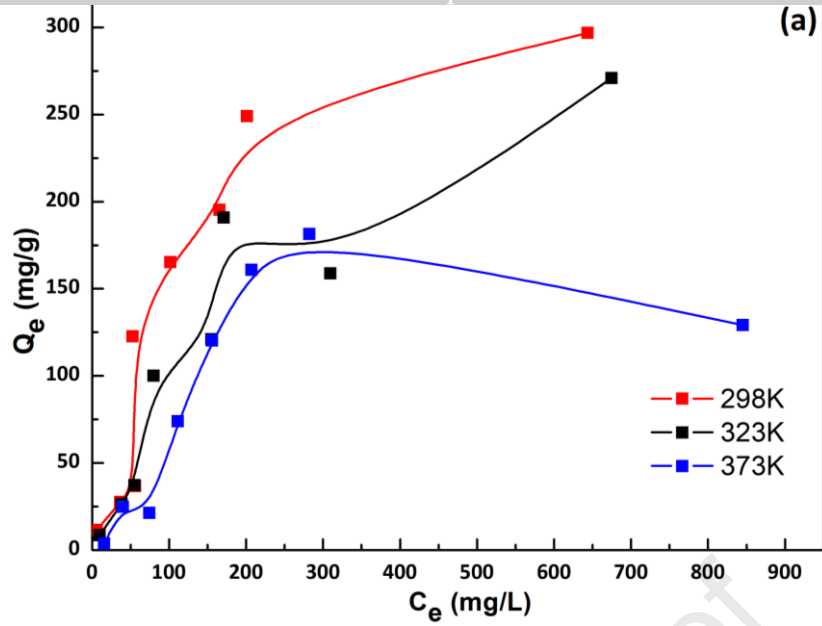


Figure 7. Adsorption Kinetics curve for the adsorption of MO on TC.



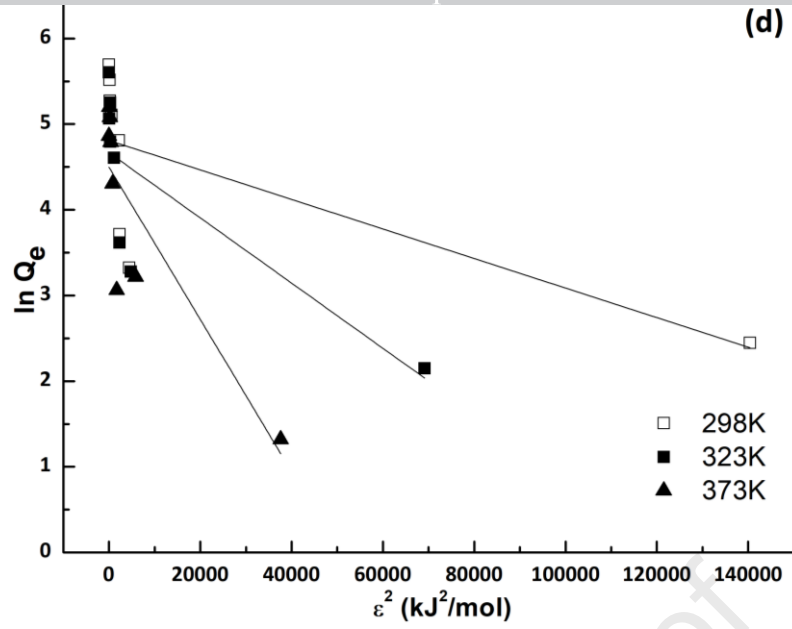


Figure 8. Adsorption isotherms of MO on TC: **(a)** at different temperatures; **(b)** Langmuir; **(c)** Freundlich; and **(d)** Dubinin-Radushkevich model.

- ✓ Clays are low-cost solids that can be used to remove colorants.
- ✓ Acid treatment of bentonite can enhance its adsorption capacity.
- ✓ Initial concentration of dye and mass of adsorbent influence adsorption capacity.
- ✓ Acid bentonite removes more than 80 % of methyl orange.

Journal Pre-proof

Declaration of interests

The authors declare that they have no known competing financial interests or personal relationships that could have appeared to influence the work reported in this paper.

The authors declare the following financial interests/personal relationships which may be considered as potential competing interests:

Signed by all authors as follows:

Maria Cecilia Avila

Ileana Daniela Lick

Nora Andrea Comelli

Maria Lucia Ruiz